Spherical Supramolecular Minidendrimers Self-Organized in an "Inverse Micellar"-like Thermotropic Body-Centered Cubic Liquid Crystalline Phase

Duncan J. P. Yeardley,[†] Goran Ungar,*[,†] Virgil Percec,*[,‡] Marian N. Holerca,[‡] and Gary Johansson[‡]

Contribution from the Department of Engineering Materials and Center for Molecular Materials, University of Sheffield, Sheffield S1 3JD, U.K., and Roy & Diana Vagelos Laboratories, Department of Chemistry, University of Pennsylvania, Philadelphia, Pennsylvania 19104-6323

Received November 4, 1999

Abstract: An "inverse micellar"- or "water-in-oil"-like (similar to the lyotropic type I_{II}) thermotropic body-centered cubic (BCC) liquid crystal (LC) phase was discovered in a poly(ethyleneimine) with a degree of polymerization (DP) = 20 containing 3,4,5-tri(dodecyloxy)benzoyl minidendritic side groups. Fiber X-ray diffraction (XRD) experiments show that the extinction symbol of this phase is *I*- - - and, alongside other evidence, suggested that the space group is $Im\bar{3}m$ (Q^{229}). These results point to a supramolecular inverse micellar-like structure with the polymer backbone and the benzoyl groups aggregated into globules located at the corners and the center of the unit cell. The *n*-alkyl groups radiate out of the aromatic part of the globule and make up the continuos matrix of the lattice. The cubic unit cell parameter is $a = 42.6$ Å. Upon shearing, the BCC phase aligns along the [111] direction. The BCC lyotropic $Im\bar{3}m$ inverse micellar phase of I_{II} type has not yet been observed and the experiments reported here will access its design. The present is only the second "inverse micellar" thermotropic LC phase known. The first one was previously reported from our laboratories (Balagurusamy, V. S. K.; Ungar, G.; Percec, V.; Johansson, G. *J. Am. Chem. Soc.* **1997**, *119*, 1539) and has a $Pm\bar{3}n$ symmetry. Both the $Im\bar{3}m$ and the $Pm\bar{3}n$ cubic lattices were self-organized from spherical supramolecular dendrimers. The BCC cubic LC lattice reported here enriches the synthetic capabilities of dendritic building blocks.

Introduction

Dendritic building blocks provide some of the most powerful synthetic tools for the design and construction of complex molecular, macromolecular, and supramolecular systems.[1] Previous publications from our laboratories have reported the design and synthesis of tapered and conical monodendrons which self-assemble into cylindrical and spherical supramolecular dendrimers. These supramolecular object-like dendrimers self-organize in 2-D hexagonal columnar *p6mm*[2,3] and 3-D cubic $Pm\bar{3}n$,[4,5,6] thermotropic liquid crystalline (LC) phases (Scheme 1). Recently, a hexagonal columnar LC superlattice was reported for a mixture of supramolecular/macromolecular minidendritic systems.[7] These latter experiments have also demonstrated the synthetic capabilities of minidendrons as models for higher generations of dendrons.[7,8] The analysis of these lattices and superlattices by X-ray diffraction experiments allows the determination of the shape and size of dendrimers[2−7] and provides access to the rational design and synthesis of functional dendritic building blocks which are required for the construction of giant nanosystems with precise shape, size, and functional

Scheme 1. Fan-Shaped and Cone-Shaped Monodendrons[a]

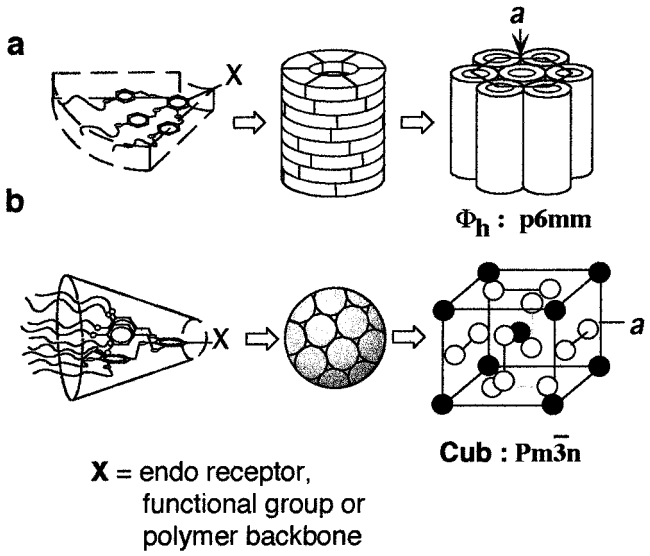

[a] Fan-shaped dendrons self-assemble into columns which self-organize in a 2-D *p6mm* hexagonal columnar LC lattice.[2d] Cone-shaped dendrons self-assemble into quasi-spherical globules which in turn pack in a $Pm\bar{3}n$ 3-D LC cubic lattice[4,5a]

[†] University of Sheffield.

[‡] University of Pennsylvania.

(1) For recent reviews on dendritic building blocks see: (a) Fréchet, J. M. *J. Science* **1994**, *263*, 1710. (b) Newcome, G. R.; Moorefield C, N.; Vogtle, F. *Dendritic Molecules*; VCH: Weinheim, 1996. (c) Moore, J. S. *Acc. Chem. Res.* **1997**, *30*, 402. (d) Tomalia, D. A.; Esfand, R. *Chem. Ind.* **1997**, 416. (e) Smith, D. K.; Diederich, F. *Chem. Eur. J.* **1998**, *4*, 1353. (f) Frey, H. *Angew. Chem., Int. Ed. Engl.* **1998**, *37*, 2193. (g) Vögtle, F., Ed. *Dendrimers*; Topics Curr. Chem. Vol. 197; Springer, Berlin, 1998. (h) Mathews, O. A.; Shipway, A. N.; Stoddart, F. *J. Prog. Polym. Sci.* **1998**, *23*, 1. (i) Fischer, M.; Vögtle, F. *Angew. Chem., Int. Ed. Engl.* **1999**, *38*, 884. (j) Bosman, A. W.; Janssen H. M.; Meijer, E. W. *Chem. Rev.* **1999**, *99*, 1665. (k) Berresheim, A. J.; Müller, M.; Müllen, K. *Chem. Rev.* **1999**, *99*, 1747. (l) Moore, J. S. *Curr. Opin. Coll. Int. Sci.* **1999**, *4*, 108. (m) Roovers, J.; Comanita, B. *Adv. Polym. Sci.* **1999**, *142*, 179.

10.1021/ja993915q CCC: $19.00
Published on Web 02/02/2000

properties in the bulk state.[9] These LC lattices are actively exploited for rational design both in our and in other laboratories.[2−8]

The goal of this publication is to report that spherical supramolecular dendrimers also self-organize into a second "inverse micellar"-like thermotropic cubic phase of $Im\bar{3}m$ space group. Both this phase and its analogue from lyotropic systems, a body-centered inverse micellar cubic phase ("water-in-oil", type I_{II}), have not actually been observed. However, the lyotropic "oil-in-water" (type I_I) analogue is known.[10]

Results and Discussion

We have selected a poly(ethyleneimine) with degree of polymerization 20 (DP = 20) containing 3,4,5-tri(dodecyloxy)-benzoyl minidendritic side groups [**poly(t12-APOX)**] to demonstrate this cubic LC phase. The present cubic phase has been observed in a large number of supramolecular dendrimers. However, we have decided to use this polymer for structural characterization because of its ability to align. The synthesis of the cyclic imino ether monomer and its living cationic ring-opening polymerization are outlined in Scheme 2. Oligo- and poly(ethyleneimine) with minidendritic side groups were investigated simultaneously in several different laboratories.[11] Most of them exhibit a hexagonal columnar LC phase.

Scheme 2. Synthesis and Polymerization of 2-[3,4,5-Tris(*n*-alkan-1-yloxy)phenyl]-2-oxazoline (**t12-APOX**)

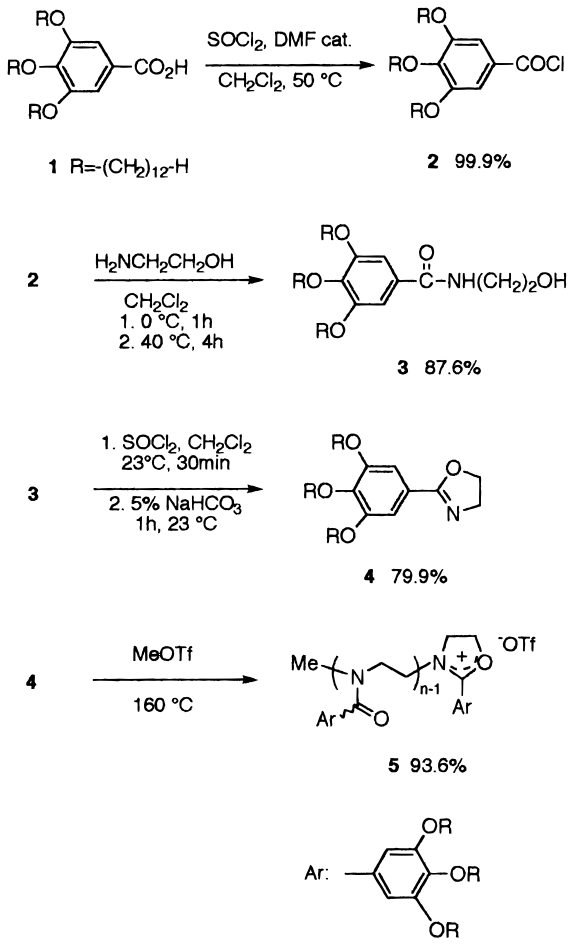

The differential scanning calorimetry trace of **poly(t12-APOX)** (Figure 1) shows two endothermic transitions on heating: one at −12 °C (ΔH = 19.5 J/g), into the thermotropic LC phase, and another at 131 °C (ΔH = 1.7 J/g), into the isotropic liquid. On cooling the reverse sequence of transitions occurs, with a small hysteresis (exothermic peaks at 122 and −16 °C). Thermal optical polarized microscopy of **poly(t12-**

(2) For selected references on cylindrical supramolecular dendrimers self-organized in hexagonal columnar LC lattices see: (a) Percec, V.; Johansson, G.; Heck, J.; Ungar, G.; Batty, S. V. *J. Chem. Soc., Perkin Trans. 1* **1993**, 1411. (b) Johansson, G.; Percec, V.; Ungar, G.; Abramic, D. *J. Chem. Soc., Perkin Trans. 1* **1994**, 447. (c) Stebani, U.; Lattermann, G. *Adv. Mat.* **1995**, *7*, 578. (d) Percec, V.; Johansson, G.; Ungar, G.; Zhou, J. *J. Am. Chem. Soc.* **1996**, *118*, 9855. (e) Pesak, D.; Moore, J. S. *Angew. Chem., Int. Ed. Engl.* **1997**, *36*, 1636. (f) Suarez, M.; Lehn, J.-M.; Zimmerman, S. C.; Skoulios, A.; Heinrich, B. *J. Am. Chem. Soc.* **1998**, *120*, 9526. (g) Meier, H.; Lehmann, M. *Angew. Chem., Int. Ed. Engl.* **1998**, *37*, 643. (h) Percec, V.; Cho, W.-D.; Mosier, P. E.; Ungar, G.; Yeardley, D. J. P. *J. Am. Chem. Soc.* **1998**, *120*, 11061. (i) Brewis, M.; Clarkson, G. J.; Holder, A. M.; McKeon, N. B. *Chem. Commun.* **1998**, 969.

(3) For selected references on cylindrical macromolecular dendrimers self-organized in hexagonal columnar LC lattices see: (a) Percec, V.; Heck.; J.; Lee, M.; Ungar, G.; Castillo, A. A. *J. Mater. Chem.* **1992**, *2*, 1033. (b) Percec, V.; Heck, J.; Tomazos, D.; Falkenberg, F.; Blackwell, H.; Ungar, G. *J. Chem. Soc., Perkin Trans. 1* **1993**, 2799. (c) Percec, V.; Heck, J. A.; Tomazos, D.; Ungar, G. *J. Chem. Soc., Perkin Trans. 2* **1993**, 2381. (d) Percec, V.; Tomazos, D.; Heck, J.; Blackwell, H.; Ungar, G. *J. Chem. Soc., Perkin Trans. 2* **1994**, 31. (e) Percec, V.; Schlueter, D.; Kwon, Y. K.; Blackwell, J.; Moller, M.; Slangen, P. J. *Macromolecules* **1995**, *28*, 8807. (f) Johansson, G.; Percec, V.; Ungar, G.; Zhou, J. P. *Macromolecules* **1996**, *29*, 646. (g) Percec, V.; Schlueter, D.; Ronda, J. C.; Johansson, G.; Ungar, G.; Zhou, J. P. *Macromolecules* **1996**, *29*, 1464. (h) Percec, V.; Schlueter, D. *Macromolecules* **1997**, *30*, 5783. (i) Percec, V.; Ahn, C.-H.; Cho, W.-D.; Jamieson, A. M.; Kim, J.; Leman, T.; Schmidt, M.; Gerle, M.; Moller, M.; Prokhorova, S. A.; Sheiko, S. S.; Cheng, S. Z. D.; Zhang, A.; Ungar, G.; Yeardley, D. J. P. *J. Am. Chem. Soc.* **1998**, *120*, 8619. (j) Prokhorova, S. A.; Sheiko, S. S.; Moller, M.; Ahn, C.-H.; Percec, V. *Macromol. Rapid Commun.* **1998**, *19*, 359. (k) Percec, V.; Schlueter, D.; Ungar, G.; Cheng, S. Z. D.; Zhang, A. *Macromolecules* **1998**, *31*, 1745. (l) Prokhorova, S. A.; Sheiko, S. S.; Ahn, C.-H.; Percec, V.; Moller, M. *Macromolecules* **1999**, *32*, 2653.

(4) For spherical supramolecular dendrimers self-organized in a $Pm\bar{3}n$ cubic LC lattice see: Balagurusamy, V. S. K.; Ungar, G.; Percec, V.; Johansson, G. *J. Am. Chem. Soc.* **1997**, *119*, 1539.

(5) For macromolecular dendrimers that change their shape from spherical to cylindrical by increasing their degree of polymerization see: (a) Percec, V.; Ahn, C.-H.; Ungar, G.; Yeardley, D. J. P.; Moller, M.; Sheiko, S. S. *Nature* **1998**, *391*, 161. (b) Yin, R.; Zhu, Y.; Tomalia, D. A. *J. Am. Chem. Soc.* **1998**, *120*, 2678.

(6) For cylindrical and spherical supramolecular dendrimers that change their shapes as a function of generation number see: (a) Hudson, S. D.; Jung, H.-T.; Percec, V.; Cho, W.-D.; Johansson, G.; Ungar, G.; Balagurusamy, V. S. K. *Science* **1997**, *278*, 449. (b) Percec, V.; Cho, W.-D.; Mosier, P. E.; Ungar, G.; Yeardley, D. J. P. *J. Am. Chem. Soc.* **1998**, *120*, 11061.

(7) For the co-assembly of a hexagonal columnar LC superlattice and the demonstration of the synthetic capabilities of minidendritic building blocks see: Percec, V.; Ahn, C.-H.; Bera, T. K.; Ungar, G.; Yeardley, D. J. P. *Chem. Eur. J.* **1999**, *5*, 1070.

(8) For additional examples of LCs generated with the aid of minidendrons see: (a) Zheng, H.; Swager, T. M. *J. Am. Chem. Soc.* **1994**, *116*, 77. (b) van Nunen, J. L. M.; Folmer, B. F. B.; Nolte, R. J. M. *J. Am. Chem. Soc.* **1997**, *119*, 283. (c) Tschierske, C. J. *J. Mat. Chem.* **1998**, *8*, 1485. (d) Pegenan, A.; Cheng, X. H.; Tschierske, C.; Goring, P.; Diele, S. *New J. Chem.* **1999**, *23*, 465.

(9) (a) Jiang, D.-L.; Aida, T. *Nature* **1997**, *388*, 454. (b) Sooklal, K.; Hanus, L. H.; Ploehn, H. J.; Murphy, C. J. *Adv. Mat.* **1998**, *10*, 1083. (c) Zhao, M.; Sun, Z. L.; Crooks, R. M. *J. Am. Chem. Soc.* **1998**, *120*, 4877. (d) Balogh, L.; Tomalia, D. A. *J. Am. Chem. Soc.* **1998**, *120*, 4877. (e) Kawa, M.; Fréchet, J. M. J. *Chem. Mater.* **1998**, *10*, 286. (f) Bao, Z.; Amundson, K. R.; Lovinger, A. J. *Macromolecules* **1998**, *31*, 8647.

(10) Gulik, A.; Delacroix, H.; Kirschner, G.; Luzzati, V. *J. Phys. II (France)* **1995**, *5*, 445.

(11) (a) Fischer, H.; Ghosh, S. S.; Heiney, P. A.; Maliszewskyj, N. C.; Plesnivy, T.; Ringsdorf, H.; Seitz, M. *Angew. Chem., Int. Ed. Engl.* **1995**, *34*, 795. (b) Fischer, H.; Plesnivy, T.; Ringsdorf, H.; Seitz, M. *J. Chem. Soc., Chem. Commun.* **1995**, 1615. (c) Stebani, U.; Latterman, G.; Festag, R.; Wittemberg, M.; Wendorff, J. H. *J. Mater. Chem.* **1995**, *5*, 2247. (d) Stebani, U.; Latterman, G. *Adv. Mat.* **1995**, *7*, 578. (e) Seitz, M.; Plesnivy, T.; Schimossek, K.; Edelmann, M.; Ringsdorf, H.; Fischer, H.; Uyama, H.; Kobayashi, S. *Macromolecules* **1996**, *29*, 6560. (f) Ungar, G.; Abramic, D.; Percec, V.; Heck, J. A. *Liq. Cryst.* **1996**, *21*, 73. (g) Johansson, G. Ph.D. Thesis Case Western Reserve University, Cleveland, OH, August 1996. (h) Percec, V.; Johansson, G.; Schlueter, D.; Ronda, J. C.; Ungar, G. *Macromol. Symp.* **1996**, *101*, 43. (i) Stebani, U.; Latterman, G.; Wittemberg, M.; Wendorff, J. H. *Angew. Chem., Int. Ed. Engl.* **1996**, *35*, 1858. (j) Fischer, H.; Plesnivy, T.; Ringsdorf, H.; Seitz, M. *J. Mater. Chem.* **1998**, *8*, 343.

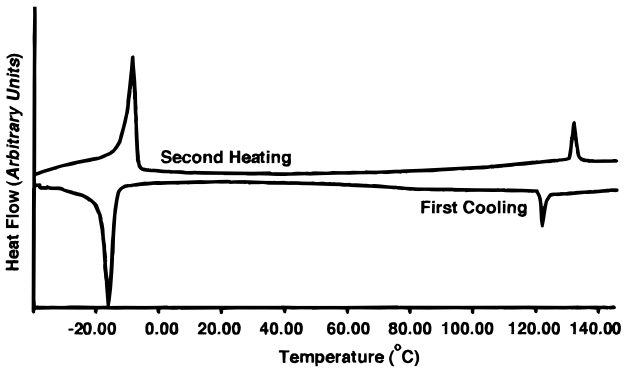

Figure 1. DSC thermograms of **poly(t12-APOX)** with DP = 20 at 10deg C per min.

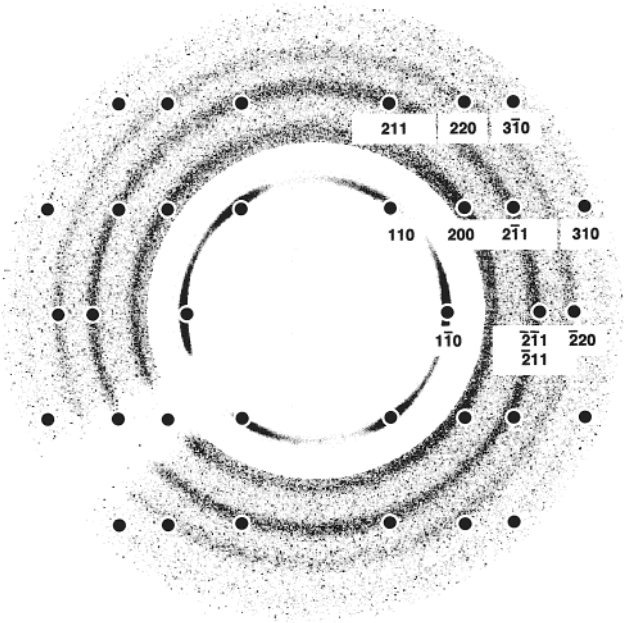

Figure 2. Low-angle X-ray fiber diffraction pattern of **poly(t12-APOX)** in the cubic phase at room temperature with an overlay of the calculated reflection positions. The inner area including {111} reflections is attenuated 100 times. The fiber axis is vertical and the preferred orientation is [111].

APOX) at room temperature shows the thermotropic mesophase to be optically isotropic. On heating, the optically isotropic texture persists in the isotropic phase. It is apparent, however, that there is a reduction in viscosity above the isotropization temperature. The optical isotropy and high viscosity of the mesophase indicates that the LC phase is most probably cubic. The crystalline phase formed below −12 °C was not analyzed by XRD.

In the wide-angle region of the X-ray diffraction pattern only a diffuse halo is observed at room temperature and above. The small-angle X-ray scattering (SAXS) fiber pattern of the partially aligned LC phase is shown in Figure 2. Only the central region is presented. The first group of reflections, arranged nearly hexagonally, are 2 orders of magnitude stronger than the next reflections. To compensate for this, the inner area of Figure 2 is attenuated by a factor of about 100. The diffraction arcs are arranged in rings with reciprocal spacings in the ratio 1:$\sqrt{2}$:$\sqrt{3}$:$\sqrt{4}$:$\sqrt{5}$ etc. (see also Table 1). The innermost reflections are consistent with a fiber sample of cubic crystals with [111] direction parallel to the fiber axis. With the first and strongest reflections indexed as {110}, indexing of the remaining reflections was consistent with the overlaid calculated diffraction

Table 1. Interplanar Spacings for XRD Reflections Observed for the Cubic LC Phase of Poly{*N*-[3,4,5-tris(*n*-dodecan-1-yloxy)benzoyl]ethyleneimine} with DP = 20

hkl	$h^2+k^2+l^2$	d_{obs}/Å	*a*/Å[a]	I_{obs}[b]
110	2	30.3	42.9	vs
200	4	21.5	42.9	s
211	6	17.4	42.7	m
220	8	15.1	42.8	m
310	10	13.5	42.7	w
222	12	12.4	42.8	w
321	14	11.4	42.5	w
400	16	10.6	42.4	w
411	18	10.0	42.4	vw
420	20	9.4	42.1	vw
332	22	9.0	42.4	w
431	24	8.7	42.6	vw

[a] Average value of unit cell parameter, $a = 42.6$ Å. [b] vs = extremely strong, s = strong, m = moderate, w = weak, vw = extremely weak.

pattern (Figure 2). This showed that only reflections obeying the conditions $0kl{:}k + l = 2n$, $hhl{:}l = 2n$, and $h00{:}h = 2n$ were present. The limited number of reflections shown in Figure 2 are not sufficient to discriminate between primitive and body-centered cubic (BCC) lattices, more precisely between the *Pn-n* and *I*--- extinction groups, respectively. The two differ by the reflection condition $hkl{:}h + k + l = 2n$, obeyed by the BCC lattice. The first set of reflections on which this condition can be tested is {421}. Diffraction patterns were recorded with long exposures and the full list of observed reflections is given in Table 1. {421} reflections are not observed, hence the assignment of extinction symbol *I*- - - could be made. The *I*- - - extinction group contains the space groups $Im\bar{3}m$, $I\bar{4}3m$, $I432$, $Im\bar{3}$, $I23$, and $I2_13$, which cannot be separated by extinctions alone. Since the Laue class could not be determined from the fiber pattern, all of the above space groups are theoretically possible. However, the following consideration makes it most unlikely that the current cubic LC phase belongs to anything but the highest symmetry space group $Im\bar{3}m$. The argument below also points to the structure and molecular organization in the present cubic mesophase.

(a) The nature of the disorder in LCs favors molecular aggregation of highest symmetry. With only one exception ($P4_3$-32, in a ternary lyotropic system),[12] all cubic LCs were found to belong to the $m\bar{3}m$ point group. When applied to the *I*- - - extinction group, this singles out the space group $Im\bar{3}m$.

(b) The taper angle of the tri(dodecyloxy) benzoyl minidendritic group used here is *too high* or just acceptable, at the high end of the range, for accommodation into infinite columns. Results to be reported soon from our laboratories have shown that in fact in most cases this building block is capable of self-assembly in spheres forming the $Pm\bar{3}n$ cubic phase. The $Pm\bar{3}n$ phase is of the "inverse micellar"-type (type I_{II} in lyotropics) rather than bicontinuous (type V). The latter forms when the interface curvature (in our case the equivalent is the molecular taper angle) is *too low* to allow the formation of the columnar phase. A "micellar" phase implies the existence of insular regions of one phase in the continuum of the other. In the thermotropic $Pm\bar{3}n$ the two microseparated subphases were made up of aromatic dendritic cores and the aliphatic end-chains, respectively.[1a,4] Since the same tapered minidendron, which previously gave rise to the $Pm\bar{3}n$ phase,[4] is used here as the polymer side group, it is most likely that the current cubic phase is also of the "inverse micellar" type. This inference is further

(12) Mariani, P.; Luzzati, V.; Delacroix, H. *J. Mol. Biol.* **1998**, *204*, 165−189.

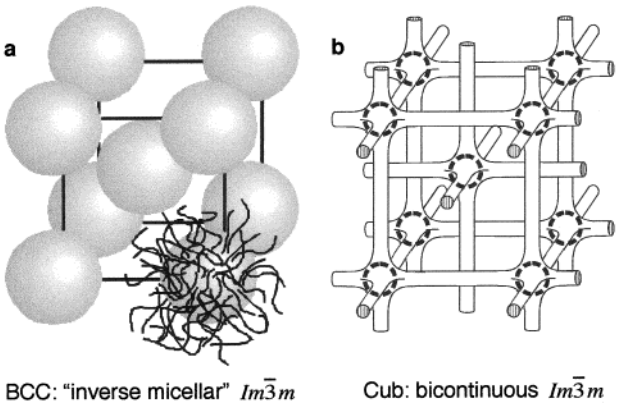

Figure 3. (a) Schematic representation of a unit cell of the "inverse micellar" (type I_{II}) $Im\bar{3}m$ **(**BCC) LC lattice. Spheres represent the preferred locations of aromatic groups and polymer backbones. The interstitial space is filled with aliphatic chains. The volume fraction of the spheres (22.5%, drawn to scale) is equal to the "aromatic" fraction of the van der Waals volume. (b) Schematic drawing of the "bicontinuous" (tube model) and "inverse micellar" variants of the $Im\bar{3}m$ cubic LC lattice. The latter structure is obtained from the former by closing off the connecting channels.

reinforced by the fact that in a number of instances this tapered minidendron exhibits the present body-centered cubic phase in addition to the $Pm\bar{3}n$.[4]

(c) 96% of the Lorentz-corrected Bragg diffraction intensity is accommodated in the {110} reflections. Consequently, if the structure factors for all {110} reflections were the same, as is the case for $Im\bar{3}m$ space group, electron density distribution is dominated by smooth, nearly spherical maxima (or minima) at positions 000 and $^1/_2,^1/_2,^1/_2$ (site symmetry $m\bar{3}m$). These special positions would be the centers of the insular domains ("micelles") of the minority subphase which, as in the $Pm\bar{3}n$ form of related compounds, is "aromatic". Including the oxygens, the poly(ethyleneimine) backbone, and the triflate anion, the "aromatic" subphase in **poly(t12-APOX)** constitutes 22.5% of the total van der Waals volume. It follows from the above that the most likely structure of the present cubic phase is the one with $Im\bar{3}m$ (Q^{229}) symmetry shown schematically in Figure 3a. The spheres at the corners and at the center of the unit cell are representative of the poly(ethyleneimine)/aromatic cores of the "inverse micelles", with the interstitial continuum filled by the aliphatic side chains in a 22.5%:77.5% volume ratio.

The relationship between the unit cell parameter ($a = 42.6$ Å) and molecular dimensions is not inconsistent with the structure in Figure 3a. Considering that the length of a fully extended side-group monomer repeat unit is ~25 Å, we find that every part of the unit cell is accessible. The furthest an alkyl chain on a monomer repeat unit anchored at the center of a "micelle" (0,0,0) must reach is position $0,^1/_2,^1/_4$ or equivalent (four per face). These positions are at a distance of 23.8 Å from the origin, hence are just reachable by extended dodecyl chains. The distance from the origin to the point closest to a neighboring "micelle" is 18.4 Å.

To set the present results in context, in the following we briefly discuss the different possible $Im\bar{3}m$ cubic structures. As already noted, there are in general two types of cubic LCs: the "micellar" I_I (normal micellar) and I_{II} (inverse micellar) type, with I_{II} being equivalent to the currently proposed structure, and the "bicontinuous" (V) type.[13] The latter occurs in lyotropic systems where either aliphatic bilayers or water subphase follow one of three infinite periodic minimum surfaces (IPMS), phase types V_{II} and V_I, respectively. The other subphase is confined to a pair of independent interpenetrating tubular networks. In the case of inverse (V_{II}) phases the buckled minimum surfaces of zero mean curvature allow bilayers to have their outer surface area slightly larger than the inner surface area. Bicontinuous phases appear in lyotropic systems close to the lamellar phase. In thermotropic compounds IPMS structures are likely when molecules have a small taper angle.

In the case of $Im\bar{3}m$ symmetry the bicontinuous type is referred to as "plumber's nightmare".[14] If we were to describe our phase in terms of an IPMS model, there would be two options: the IPMS is defined either by the methyl groups at the ends of the alkyl chains (inverse cubic, V_{II}) or by the polymer backbone (normal cubic, V_I). The analogy with the lyotropic classification is based here on water being replaced by the poly(ethyleneimine)/aromatic subphase. If the polymer backbones were located at the minimum surface, alkyl chains would have to converge to singularities at 0,0,0 and $^1/_2,^1/_2,^1/_2$. This is contrary to the geometry of the tapered monodendritic group with three divergent alkyl chains. On the other hand, the first option, whereby the methyl groups are near the IPMS, is compatible with molecular geometry.

The distinction between "bicontinuous" and "micellar" $Im\bar{3}m$ phases is illustrated in Figure 3b. For clarity the tube model is used to represent schematically the bicontinuous phase. The minimum surface is not drawn. Referring to the inverse phases, water or polymer backbones are confined to the tubes in the bicontinuous cubic phase, and to isolated spheres in the case of the micellar phase. In the lyotropic case, the main parameter determining whether the phase is bicontinuous or micellar is the volume fraction of water. In the case of thermotropic systems such as ours, in addition to the aromatic volume fraction there are other dominant parameters of molecular architecture at play, such as the number and type of pendant chains, structure of the dendritic core, degree of polymerization in the case of polymers, etc. The bicontinuous thermotropic LC phase of $Im\bar{3}m$ symmetry is known.[15] It involves molecules with very small taper that are liable to form bilayers.

The inverse lyotropic micellar $Im\bar{3}m$ phase ("water-in-oil", type I_{II}) has not been reported so far, whereas the normal micellar one (type I_I) has.[10] Only one type of inverse micellar (type I_{II}) cubic phase, with $Fd\bar{3}m$ symmetry, has been found so far in lyotropic systems.[16,17]

The field of block copolymers has also contributed to the discovery of phase separated cubic morphologies.[18] A "micellar" type $Im\bar{3}m$ phase was first shown by electron microscopy in a triblock copolymer[19] and later by neutron scattering in a diblock

(13) Seddon, J. M. *Biochem. Biophis. Acta* **1990**, *1031*, 1−69.

(14) Seddon, J.; Temple, R. *New Scientist* **1991**, *130*, 45.

(15) For a recent review on thermotropic cubic phases see: (a) Diele, S.; Göring, P. In *Handbook of Liquid Crystals*; Demus, D., Goodby, J., Gray, G. W., Spiess, H.-W., Vill, V., Eds.; Wiley-VCH: Weinheim, 1998; Vol. 2B, pp 887−900. For several examples of thermotropic bicontinuous cubic LC phase of $Im\bar{3}m$ symmetry see: (b) Levelut, A. M.; Fang, Y. *J. Phys. Colloq. France* **1990**, *51*, Suppl. C7229. (c) Kutzumizu, S.; Ichikawa, T.; Nojima, S.; Yano, S. *Chem. Commun.* **1999**, 1181.

(16) Luzzati, V.; Vargas, V.; Gulik, A.; Mariani, P.; Seddon, R. M.; Rivas, E. *Biochemistry* **1992**, *31*, 279.

(17) Seddon, J. M.; Zeb, N.; Templer, R. H.; McElhaney, R. N.; Mannock, D. A. *Langmuir* **1996**, *12*, 5250.

(18) For several representative publications on complex phase behavior in block copolymers see, for example: (a) Bates, F. S. *Science* **1991**, *25*, 898. (b) Hillmyer, M. A.; Bates, F. S.; Almdal, K.; Mortensen, K.; Ryan, A. J.; Fairclough, J. P.A *Science* **1996**, *271*, 976. (c) Fredrikson, G. H.; Bates F. S. *Annu. Rev. Mater. Sci.* **1996**, *26*, 501. (d) Thomas, E. L.; Anderson, D. M.; Henkee, C. S.; Hoffman, D. *Nature* **1988**, *334*, 598. (e) Shefelbine, T. A.; Vigild, M. E.; Matsen, M. W.; Hajduk, D. A.; Hillmyer, M. A.; Cussler, E. L.; Bates, F. S. *J. Am. Chem. Soc.* **1999**, *121*, 8457.

(19) Pedemonte, E.; Turturro, A.; Bianchi, U.; Devetta, P. *Polymer* **1973**, *14*, 145.

compound.[20] However, although the "micellar"-type $Im\bar{3}m$ phase from block copolymers is considered from the symmetry point of view similar to the thermotropic $Im\bar{3}m$ LC phase, it cannot be differentiated into "inverse" (type I_{II}) and "normal" (type I_I) "micellar", as is possible in the case of lyotropic LCs and of the LC phase reported here.

Returning to the present system, there are 3.2 **poly(t12-APOX)** macromolecules with $M_w/M_n = 1.11$ per unit cell, or 1.6 per "micelle", for an experimental density of 0.95 g/cm^3. However, this density was obtained from a sample that was not annealed to perfect crystallinity and consequently it is lower than that of the highly ordered lattice sampled by XRD. Therefore, it would appear that in most cases two macromolecules self-assemble into a spherical object. By analogy with the spherical polymers containing dendritic side groups which self-organize in a $Pm\bar{3}n$ cubic phase,[5a] in the present case the polymer backbones are also believed to be coiled within the interior of the "micelle".

Conclusions

Poly{*N*-[3,4,5-tris(*n*-dodecan-1-yloxy)benzoyl]ethyleneimine} with DP = 20 displays an "inverse micellar" (type I_{II}-like) body-centered cubic (BCC) LC phase. A multitude of evidence indicates that the space group is $Im\bar{3}m$ (Q^{229}). Two macromolecules pair up to form "inverse micellar"-like objects with globular cores centered at 0,0,0 and $^1/_2,^1/_2,^1/_2$ positions and containing polymer backbones and aromatic groups (Figure 3a). As in the case of $Pm\bar{3}n$ cubic LC lattice discovered previously in our laboratories,[4,5a,6] in the present case the *n*-alkyl side chains also radiate out of the aromatic core and make up the continuous matrix. The globular supramolecular minidendrimer contains approximately forty 3,4,5-tri(dodecyloxy)benzoyl minidendritic groups. We have observed the present cubic phase in a large number of other spherical supramolecular dendrimers. As expected, the shear alignment of this phase is along the [111] direction, i.e., the direction of closest packing of "micelles". This "inverse micellar" $Im\bar{3}m$ thermotropic LC phase expands our capabilities to design and construct functional nanoobjects from dendritic building blocks. It also provides synthetic strategies for the design of the lyotropic $Im\bar{3}m$ inverse micellar cubic phase (type I_{II}) that was not yet reported. The results reported here provide access to the investigation of the similarities and differences between the spherical supramolecular dendrimers which self-organize in $Pm\bar{3}n$ (Scheme 1b) and $Im\bar{3}m$ (Figure 3a) cubic lattices and to the elucidation of the mechanism that determines the selection of one of these two lattices.

Experimental Section

Materials. Hexanes (Fisher, A.C.S. reagent) was used as received. THF (Fisher, A.C.S. reagent) was refluxed over sodium ketyl and freshly distilled before use. CH_2Cl_2 (Fisher, A. C. S. reagent) was refluxed over CaH_2 and freshly distilled before use. Benzene (Fisher, ACS reagents) was shaken with concentrated H_2SO_4, washed twice with water, dried over $MgSO_4$, and finally distilled over CaH_2 or sodium ketyl, respectively. Dimethylformamide (DMF), KOH, K_2CO_3, and $NaHCO_3$ (all Fisher, A.C.S. reagents) were used as received. $SOCl_2$ (97%), 3,4,5-trihydroxybenzoic acid (97%), ethanolamine (EtOH) (99+%), and $LiAlH_4$ (95+%) (all from Aldrich) were used as received. 1-Bromododecane (98+%) (Lancaster) was used as received. Methyl trifluoromethanesulfonate (MeOTf) (Fluka, ≥97%) was freshly distilled under vacuum before use.

General Methods. ^{1}H NMR (200 MHz) and ^{13}C NMR (50 MHz) spectra were recorded on a Varian Gemini 200 spectrometer. $CDCl_3$ was used as solvent and TMS as internal standard unless otherwise noted. Chemical shifts are reported as δ, ppm. The purity of products was determined by a combination of techniques including thin-layer chromatography (TLC) on silica gel plates (Kodak) with fluorescent indicator and high-pressure liquid chromatography (HPLC). HPLC measurements were carried out by using a Perkin-Elmer Series 10 high-pressure liquid chromatograph equipped with an LC-100 column oven, Nelson Analytical 900 Series integrator data station, and two Perkin-Elmer PL gel columns of 5×10^2 and 1×10^4 Å. THF was used as solvent at the oven temperature of 40 °C. Detection was by UV absorbance at 254 nm. Weight average (M_w) and number average (M_n) molecular weights were determined with the same instrument and a calibration plot constructed from polystyrene standards. M_n was also determined from the ^{1}H NMR analysis of the polymer chain ends. Thermal transitions of samples that were freeze-dried from benzene were measured on a Perkin-Elmer DSC-7 differential scanning calorimeter (DSC). In all cases, the heating and cooling rates were 10 °C min^{-1} unless otherwise noted. First-order transition temperatures were reported as the maxima and minima of their endothermic and exothermic peaks. Glass transition temperatures (T_g) were read at the middle of the change in heat capacity. Indium and zinc were used as calibration standards. An Olympus BX-40 optical polarized microscope (100× magnification) equipped with a Mettler FP 82 hot stage and a Mettler FP 80 central processor was used to verify thermal transitions and characterize anisotropic textures.

X-ray diffraction (XRD) experiments were performed using an Image Plate area detector (MAR Research) with a graphite-monochromatized pinhole-collimated Cu Kα beam and a helium tent. XRD experiments were also performed at several small-angle stations of the Synchotron Radiation Source at Daresbury, UK. A double-focused beam and a quadrant detector were used. In both cases the sample was held in a capillary within a custom-build temperature cell controlled to within ±0.1 °C. Capillaries holding the dried samples were sealed under nitrogen. Elemental analysis was carried out at MHW Laboratories, Phoenix AZ. Densities (ρ_{20}) were determined by flotation in gradient columns at 20 °C.

Synthesis. 3,4,5-Tris(*n*-dodecan-1-yloxy)benzoic acid was synthesized as previously reported.[2a]

3,4,5-Tris(*n*-dodecane-1-yloxy)benzoyl chloride (2).[11f] 3,4,5-Tris(*n*-dodecan-1-yloxy)benzoic acid (20.5 g, 30.4 mmol) was suspended in 250 mL of CH_2Cl_2 and a catalytic amount of DMF was added. $SOCl_2$ (7.3 g, 60.75 mmol) was added dropwise and the mixture was heated to reflux for 1.5 h. After cooling to room temperature, the solvent and the excess of $SOCl_2$ were distilled to yield 20.3 g (99.9%) of a white powder that was used without further purification. ^{1}H NMR ($CDCl_3$, δ, ppm, TMS): 0.88 (overlapped t, 9H, C*H*$_3$), 1.26 (m, 54H, CH$_3$-(C*H*$_2$)$_9$), 1.78 (m, 6H, C*H*$_2$CH$_2$OAr), 4.02 (t, 4H, C*H*$_2$OAr, 3,5-position, J = 6.2 Hz), 4.08 (t, 2H, C*H*$_2$OAr, 4-position, J = 6.2 Hz), 7.33 (s, 2H, Ar).

***N*-[3,4,5-Tris(*n*-dodecan-1-yloxy)benzoyl]-2-aminoethanol (3).**[11g] Compound **2** (17.63 g, 25.45 mmol) was dissolved in 400 mL of CH_2Cl_2 and slowly added to ice-cooled ethanolamine (25 mL) under vigorous stirring. The mixture was stirred at 0 °C for 1 h and then the temperature was raised to 40 °C for another 4 h. The solution was poured into a separatory funnel and washed three times with H_2O, dried over $MgSO_4$, and filtered. The solvent was removed by rotary evaporation and the crude product was recrystallized twice from acetone at 0 °C to yield 16.08 g (87.6%) of a white powder, mp 68−70 °C. Purity (HPLC), 99+%; TLC (1:1 hexanes:EtOAc), R_f = 0.42. ^{1}H NMR ($CDCl_3$, δ, ppm, TMS): 0.88 (t, 9H, C*H*$_3$, J = 6.3 Hz), 1.27−1.65 (m, 54H, CH$_3$(C*H*$_2$)$_9$), 1.78 (m, 6H, C*H*$_2$CH$_2$OAr), 2.68 (bs, 1H, O*H*), 3.62 (q, 2H, C*H*$_2$OH, J = 4.5 Hz) 3.83 (t, 2H, NHC*H*$_2$, J = 4.8 Hz), 3.99 (overlapped t, 6H, C*H*$_2$OAr), 6.53 (m, 1H, CON*H*), 6.97 (s, 2H, Ar). ^{13}C NMR ($CDCl_3$, δ, ppm): 14.1 (*C*H$_3$), 22.7 (CH$_3$*C*H$_2$), 26.1 (*C*H$_2$-CH$_2$CH$_2$O), 29.4, 29.6 (CH$_3$CH$_2$CH$_2$(*C*H$_2$)$_6$), 30.3 (*C*H$_2$CH$_2$OAr), 31.9 (CH$_3$CH$_2$*C*H$_2$), 43.0 (NH*C*H$_2$), 62.5 (*C*H$_2$OH), 69.3 (*C*H$_2$OAr, 4-position), 73.4 (*C*H$_2$OAr, 3,5-position), 105.7 (*ortho* to O), 128.9 (*ipso* to CONH), 140.8 (*para* to CONH), 153.1 (*meta* to CONH), 168.4 (*C*ONH).

2-[3,4,5-Tris(*n*-dodecan-1-yloxy)phenyl]-2-oxazoline (4).[11g] Compound **3** (15 g, 21 mmol) and a catalytic amount of DMF were dissolved

(20) Bates, F. S.; Cohen, R. E.; Berney, C. V. *Macromolecules* **1982**, *15*, 589.

in 250 mL of CH_2Cl_2 and $SOCl_2$ (15.25 mL, 0.21 mol) was added dropwise. After 0.5 h, ^{1}H NMR as well as TLC (1:1 hexanes:EtOAc) analysis indicated complete consumption of **3.** The reaction was neutralized by addition of 400 mL of saturated $NaHCO_3$ solution accompanied by vigorous stirring of the two-phase system for 1 h. The organic layer was separated, washed three times with 200 mL of water, dried over $MgSO_4$, and filtered. The solvent was removed on a rotary evaporator and the product was recrystallized twice from hexanes at 0 °C to yield 11.54 g (79.9%) of a white solid, mp 50−52 °C. Purity (HPLC), 99+%; TLC (CH_2Cl_2), $R_f = 0.30$. ^{1}H NMR ($CDCl_3$, δ, ppm, TMS): 0.88 (t, 9H, CH_3, $J = 6.3$ Hz), 1.26 (m, 54H, $CH_3(CH_2)_9$), 1.77 (m, 6H, CH_2CH$_2$OAr), 4.00 (t, 6H, CH_2OAr, $J = 6.5$ Hz), 4.04 (t, 2H, OCH$_2$CH_2N, $J = 10.0$ Hz), 4.42 (t, 2H, OCH_2CH$_2$N, $J = 9.5$ Hz), 7.15 (s, 2H, Ar). ^{13}C NMR ($CDCl_3$, δ, ppm): 14.1 (*C*H$_3$), 22.7 (CH$_3$*C*H$_2$), 26.1 (*C*H$_2$CH$_2$CH$_2$OAr), 29.3, 29.6 (CH$_3$CH$_2$CH$_2$(*C*H$_2$)$_6$), 30.3 (*C*H$_2$CH$_2$OAr), 31.9 (CH$_3$CH$_2$*C*H$_2$), 54.9 (N*C*H$_2$), 67.6 (═CO*C*H$_2$), 69.1 (*C*H$_2$OAr, 4-position), 73.4 (*C*H$_2$OAr, 3,5-position), 106.6 (*ortho* to O), 122.4 (*ipso* to C), 140.9 (*para* to C), 152.9 (*meta* to C), 164.6 (*C*═N). Anal. Calcd for $C_{45}H_{81}O_4N$: C, 77.19, H, 11.66. Found: C, 76.97, H, 11.76.

Poly{*N*-[3,4,5-Tris(*n*-dDodecan-1-yloxy)benzoyl]ethyleneimine} [poly(t12-APOX), 5].[11g] A Schlenk tube equipped with a magnetic stirrer was dried at 180 °C overnight and charged with **4** (0.30 g, 0.43 mmol). The monomer was dissolved in 1 mL of benzene and freeze-dried in the septum-sealed Schlenk tube. After freeze-drying, the Schlenk tube was flushed with Ar. The initiator MeOTf (3.51 mg, 0.021 mmol) was added under a stream of N_2 via a syringe. The Schlenk tube was immersed in an oil bath that was preheated to 160 °C and stirred. After 60 min the monomer conversion was higher than 99% (HPLC). The polymerization was cooled to room temperature and diluted with 2 mL of CH_2Cl_2, then the polymer was precipitated in cold acetone, filtered, dried, redissolved in benzene and freeze-dried. Yield 92.3%. $M_{n,th} = 14140$, $M_{n,NMR} = 12050$, $M_{n,GPC} = 9010$, $M_n/M_w = 1.11$. $\rho_{20} = 0.95$ g/cm^3. ^{1}H NMR ($CDCl_3$, δ, ppm, TMS): 0.88 (m, CH_3), 1.26−2.00 (m, CH$_3$(CH_2)$_{11}$), 2.86−3.5 (br, NCH_2CH_2N, NCH_3), 3.8−4.0 (br, CH_2OAr), 6.38−6.82 (br, Ar).

Acknowledgment. Financial support from the National Science Foundation (DMR-97-08581) and the Engineering and Physical Science Research Council (UK) are gratefully acknowledged. We thank Professor S. Z. D. Cheng from Akron University for the density measurements.

JA993915Q